

Model Structure of the Na⁺/H⁺ Exchanger 1 (NHE1) FUNCTIONAL AND CLINICAL IMPLICATIONS^{*[5]}

Received for publication, July 3, 2007, and in revised form, October 24, 2007. Published, JBC Papers in Press, November 2, 2007, DOI 10.1074/jbc.M705460200

Meytal Landau[‡], Katia Herz[§], Etana Padan^{§1}, and Nir Ben-Tal^{‡2}

From the [‡]Department of Biochemistry, George S. Wise Faculty of Life Sciences, Tel-Aviv University, 69978 Tel-Aviv and the [§]Department of Biochemistry, Alexander Silberman Institute of Life Sciences, The Hebrew University of Jerusalem, 91904 Jerusalem, Israel

Eukaryotic Na⁺/H⁺ exchangers are transmembrane proteins that are vital for cellular homeostasis and play key roles in pathological conditions such as cancer and heart diseases. Using the crystal structure of the Na⁺/H⁺ antiporter from *Escherichia coli* (EcNhaA) as a template, we predicted the three-dimensional structure of human Na⁺/H⁺ exchanger 1 (NHE1). Modeling was particularly challenging because of the extremely low sequence identity between these proteins, but the model structure is supported by evolutionary conservation analysis and empirical data. It also revealed the location of the binding site of NHE inhibitors; which we validated by conducting mutagenesis studies with EcNhaA and its specific inhibitor 2-aminoperimidine. The model structure features a cluster of titratable residues that are evolutionarily conserved and are located in a conserved region in the center of the membrane; we suggest that they are involved in the cation binding and translocation. We also suggest a hypothetical alternating-access mechanism that involves conformational changes.

Sodium/hydrogen transporters are ubiquitous transmembrane (TM)³ proteins that transport Na⁺ and H⁺ ions across the membrane, and are therefore imperative for vital cellular processes such as regulation of cellular pH, cell volume, and ion composition (1). The mammalian Na⁺/H⁺ exchanger (NHE) family of transporters includes nine isoforms (NHE1 through NHE9), of which NHE1 is the most widely expressed. Following allosteric activation by intracellular acidification, NHE1 exchanges extracellular Na⁺ for intracellular H⁺ with Na⁺:H⁺ stoichiometry of 1:1 (2). NHE1 is inhibited by amiloride and its derivatives and by benzoyl guanidium compounds such as cariporide (1). Structurally, NHE1 is predicted to include two distinct domains: a TM N-terminal region of ~500 amino acids that is involved in ion translocation and drug recognition, and a

cytoplasmic regulatory C-terminal domain of nearly 300 residues (3). The cytoplasmic domain includes the H⁺ sensor and also serves to mediate regulation by other molecules or ions.

NHE1 is associated with many pathological conditions that include cancer as well as heart, vascular, gastric, and kidney diseases (1, 2). For example, the activity of NHE1 is primarily involved in the damage inflicted on the human myocardium during and following a myocardial infarction, and accordingly, NHE1 inhibitors were shown to be beneficial during ischemia and reperfusion (1). In addition, NHE1 plays a role in tumor growth by reversing the pH gradient in malignant cells, a phenomenon known as “malignant acidosis,” which is a key step in oncogenic transformation. Therefore, NHE1 inhibitors can potentially serve as anti-cancer drugs (1).

NhaA, the main Na⁺/H⁺ antiporter in *Escherichia coli* (EcNhaA), is indispensable for bacterial growth in alkaline pH (in the presence of Na⁺) and for adaptation to high salinity (4). EcNhaA is an electrogenic antiporter extracting one Na⁺ ion from the cell in return for inward current of two protons following cellular alkalization (4). The function of EcNhaA is specifically inhibited by 2-aminoperimidine (AP), a guanidine-containing naphthalene derivative with some similarity to the NHE1 inhibitor amiloride (5). The three-dimensional structure of EcNhaA was recently determined, and found to comprise 12 TM segments (6).

The bacterial EcNhaA and eukaryotic Na⁺/H⁺ exchangers play similar roles in controlling pH and electrolyte homeostasis, and have been suggested to share a common ancestor and a similar structural fold (1, 7). Thus, our working hypothesis was that EcNhaA can be utilized as a template to predict the structure of the TM domain of NHE1. However, the proteins share very low sequence identity of about 10%, and it is not a simple matter to align their sequences and to predict the structure of NHE1 based on that of EcNhaA (8). In this study, by using a fold-recognition approach, we obtained a three-dimensional model of NHE1. Notably, the membrane topology of this model structure differs from the one that was suggested on the basis of hydrophobicity scales and cysteine accessibility analysis (9). Reasons for the differences are discussed below.

Our model of NHE1, which is supported by both phylogenetic and empirical data, incorporates the binding pocket of clinically important NHE inhibitors. This allowed us to locate the binding site of the AP inhibitor within the EcNhaA structure by site-directed mutagenesis. Finally, the integration of empirical data with the new structural model allowed us to suggest an alternating-access mechanism of the Na⁺/H⁺ exchange in molecular detail (Fig. 1A).

* This work was supported in part by Grant 222/04 from the Israel Science Foundation (to N. B.-T.). The costs of publication of this article were defrayed in part by the payment of page charges. This article must therefore be hereby marked “advertisement” in accordance with 18 U.S.C. Section 1734 solely to indicate this fact.

[5] The on-line version of this article (available at <http://www.jbc.org>) contains supplemental Methods, Tables 15–25, Figs. 1S–4S, and additional references.

¹ Supported by Israel Science Foundation Grant 501/03-16.2, USA-Israel Binational Science Foundation (BSF) Grant 2005013, and the German-Israeli Foundation (GIF) for Scientific Research and Development.

² To whom correspondence should be addressed. Tel.: 972-3-6406709; Fax: 972-3-6406834; E-mail: bental@ashtoret.tau.ac.il.

³ The abbreviations used are: TM, transmembrane; EcNhaA, Na⁺/H⁺ antiporter from *Escherichia coli*; NHE1, Na⁺/H⁺ exchanger isoform 1; AP, aminoperimidine; MSA, multiple sequence alignment.

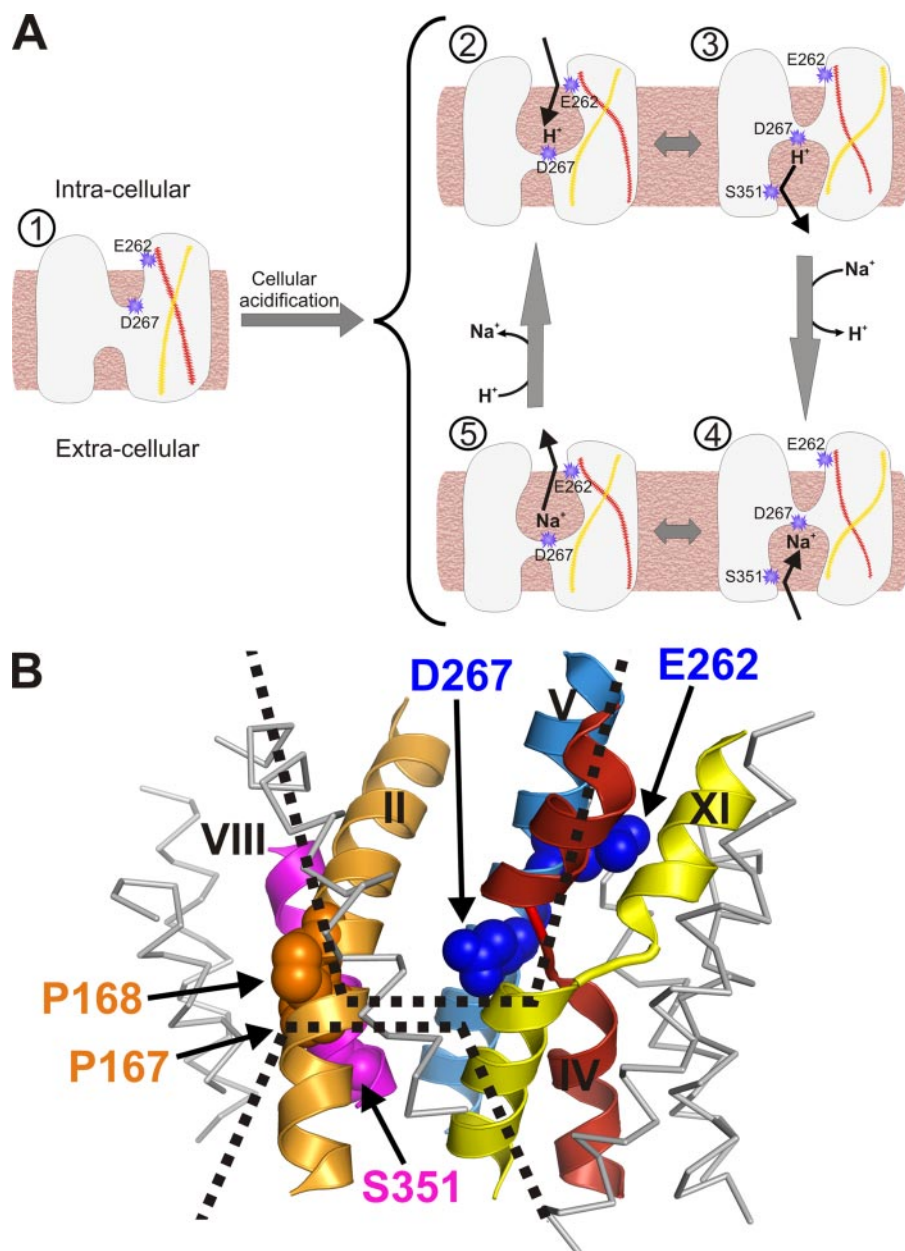


FIGURE 1. A suggested Na^+/H^+ exchange mechanism of NHE1. *A*, state 1 represents an inactive conformation, and the exchange cycle (states 2–5) illustrates putative conformational changes in the TM domain that follow activation by cellular acidification. The cycle involves dynamic equilibrium between conformations 2 and 5, in which the cation-binding site is accessible to the cytoplasm, and conformations 3 and 4, in which it is accessible to the extracellular matrix. The changes are mediated by the TM4–TM11 assembly and may also involve rotation of TM8 and exposure of Ser³⁵¹ to the extracellular funnel (indicated in states 3 and 4). The cycle allows the transport of cations across the membrane via an alternating-access mechanism. In state 2, low pH promotes the entrance of a proton to the cytoplasmic funnel, probably attracted by the acidic Glu²⁶², and the protonation of Asp²⁶⁷. The low pH also induces conformational changes, leading to the transfer of the proton from the cytoplasmic funnel to the extracellular funnel (state 3). In accordance with the chemical gradient of both cations, the proton is exchanged for sodium ion in the extracellular matrix, perhaps via Ser³⁵¹ (state 4). Finally, movements to the alternative conformation (state 5) allows the replacement of sodium by a proton at the cytoplasmic side (state 2), again in accordance with their chemical gradients. The continuance of the cycle is controlled by cellular pH. *B*, the model structure of the TM domain of NHE1 in the inactive conformation of state 1 viewed from the membrane. The intracellular side is facing upward. TM segments that are important for function are represented by the colored ribbons. Other segments are represented by a gray trace. TM1 was omitted for clarity. Residues involved in the cation transport path are represented by space-filled atoms. The funnels laying the transport path are indicated by dashed lines.

MATERIALS AND METHODS

Evolutionary Conservation Analysis of the NhaA Na^+/H^+ Antiporter Family—Calculation of evolutionary conservation scores was based on a multiple sequence alignment (MSA) of 94

sequences of bacterial NhaA Na^+/H^+ antiporters using a Bayesian method (10). The scores were mapped onto the three-dimensional structure of EcNhaA (Protein Data Bank entry 1ZCD (6)) using the ConSurf web server (consurf.tau.ac.il/) (11). The procedure used to construct the MSA is described in the supplemental data.

Evolutionary Conservation Analysis of NHE1-related Na^+/H^+ Exchangers—Calculation of evolutionary conservation scores was based on an MSA of 305 sequences of Na^+/H^+ exchangers using a Bayesian method (10). Scores were mapped onto the three-dimensional model of NHE1 using the ConSurf web server (consurf.tau.ac.il/) (11). The procedure used for MSA construction is described in the supplemental data.

Construction of Three-dimensional Model Structure—Modeling of the structure of NHE1 (SwissProt entry SL9A1_HUMAN), residues 126–505, was based on the template structure of EcNhaA (6), using the homology modeling program NEST (12) with default parameters. The final model was based on the pairwise alignments constructed as described under “Results.”

Experimental Procedure—EP432 cells transformed with plasmids encoding the various EcNhaA variants were grown. Everted membrane vesicles were prepared and used to determine the Na^+/H^+ antiporter activity. The procedures are described in the supplemental data.

Figures—Figs. 1B, 3B, 4, 5, and 6B were drawn with PyMol (39) (www.pymol.org).

RESULTS

EcNhaA and Eukaryotic Na^+/H^+ Exchangers Share a Similar Fold

Using the sequence of NHE1 as a target, we detected EcNhaA as the closest homologue according to the fold-recognition FFAS03 server (13). This finding strengthened our working hypothesis that the TM domains of the two exchangers share a similar fold.

Three-dimensional Model of NHE1 and Functional Implications

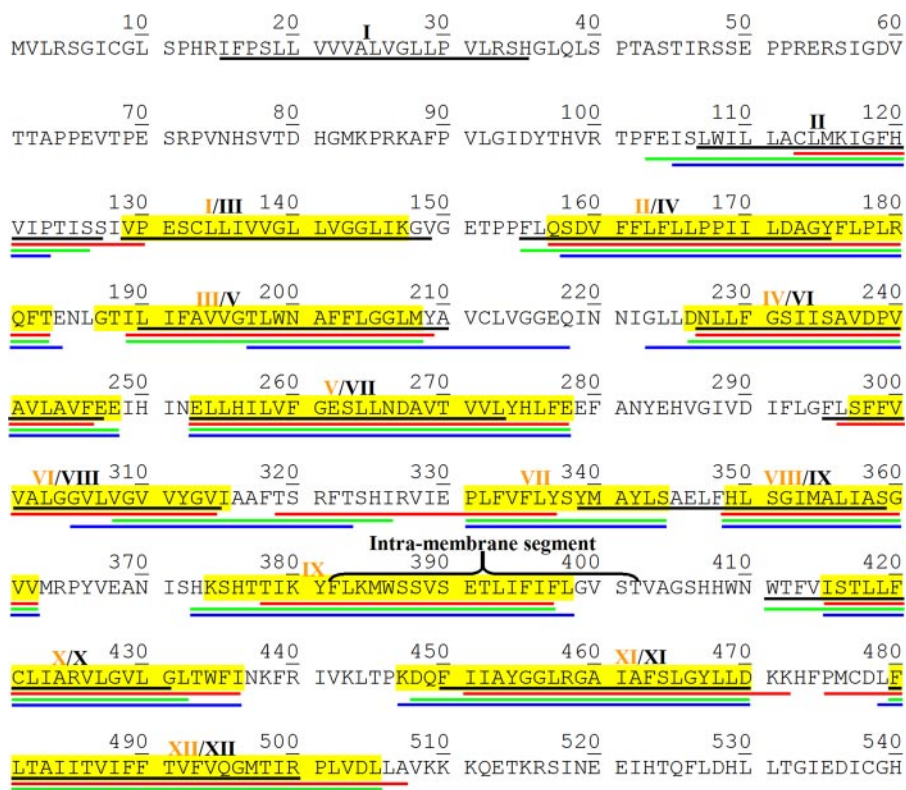


FIGURE 2. **The TM segments in the NHE1 sequence.** The segments in NHE1 that correspond to the TM helices in EcNhaA, as predicted by the different methods discussed in the main text, are *underlined* on the sequence of NHE1 (residues 1–540) as follows: for Pfam’s prediction, *red*; FFAS03 in *green*, and HMAP in *blue*. The boundaries of the TM segments as previously predicted (9), as well as their numbering, are indicated by *black lines* and *Roman numerals*, respectively. The segment predicted by Wakabayashi and co-workers (9) to be intra-membranal is also indicated. The final helix assignment proposed here is highlighted in *yellow* and the numbering of the TM helices is indicated by the *orange Roman numerals*. The overall consensus between the methods is evident. The reasons for the selection of the location of TM1 are discussed in the main text.

Predicting the Topology of NHE1

Use of Multiple Approaches to Align the TM Domains of NHE1 and EcNhaA—The sequence identity between EcNhaA and human NHE1 is only ~10%, and we were unable to align their sequences using standard methods (data not shown). We therefore used several state-of-the-art approaches to construct alignments, and integrated the results. First, we extracted the pairwise alignment between NHE1 and EcNhaA, which displays 12.4% sequence identity, from a multiple-sequence alignment of a clan of transporters from the Pfam data base (14). Two additional pairwise alignments were calculated using the FFAS03 (13) and HMAP (15) servers, which display 9.2 and 10.4% sequence identity, respectively. The procedures are described in the supplemental data.

TM Helix Assignment—We used each of the above alignments to assign the boundaries of 12 TM segments (TM1–TM12) of NHE1, based on corresponding segments of the crystal structure of EcNhaA. Fig. 2 exemplifies the significant similarity between most of the TM segments predicted by the Pfam, FFAS03, and HMAP alignments. Using the iterative process described below, we predicted the final membrane topology (highlighted in *yellow* in Fig. 2 and illustrated in Fig. 3A).

Initially, the three different alignments were manually adjusted to reduce gaps in the TM helices of EcNhaA, and used

to build three-dimensional models of NHE1. The main dissimilarity between the different alignment methods appeared to be in the prediction of the TM6 and TM7 segments. The model structures provided additional information that was used to favor a specific assignment and improve it further; model structures that were favored were those with least polar residues facing the lipid bilayer. Such considerations favored adaptation of the Pfam assignment of TM6; they were not helpful, however, in assigning TM7, for which we therefore used information from a multiple-sequence alignment of homologous eukaryotic Na^+/H^+ exchangers. Because TM helices are expected not to include insertions and deletions of amino acids (8), we favored the assignment of TM7 to a gap-free region, as predicted by FFAS03 and HMAP alignments but not by Pfam. Similar reasoning led us to reject the assignment of the first TM segment to residues 103–127, although that was the assignment predicted by all three methods (Fig. 2), because this segment is highly variable and includes many insertions and deletions. In contrast, the next segment

(residues 129–150), which was predicted by hydrophobicity analysis (9) to be a TM segment, is devoid of gaps. Interestingly, the conservation pattern in this region is compatible with the periodicity of a helix, *i.e.* a conserved residue appears at every fourth position, resulting in a conserved helical face (Fig. 3A). Accordingly, this was the region to which we assigned TM1.

Building the Three-dimensional Model of NHE1

The above helix assignment of NHE1 was used to refine the pairwise alignment between NHE1 and EcNhaA in the TM regions. The final pairwise alignment displays 10.6% sequence identity (supplemental data Fig. 1S). A three-dimensional model of NHE1 was subsequently constructed on the basis of this alignment and the EcNhaA template. An analysis pertaining to the three-dimensional location of the identical residues between NHE1 and EcNhaA is presented in the supplemental data.

Assessment of the Three-dimensional Model

The Three-dimensional Model of NHE1 Is Compatible with Evolutionary Conservation Analyses of Na^+/H^+ Exchangers—In helical proteins, evolutionarily conserved amino acids are typically located in strategic regions at the interfaces between the TM segments, whereas variable residues face the membrane lipids. The extra-membranal loops are also enriched in

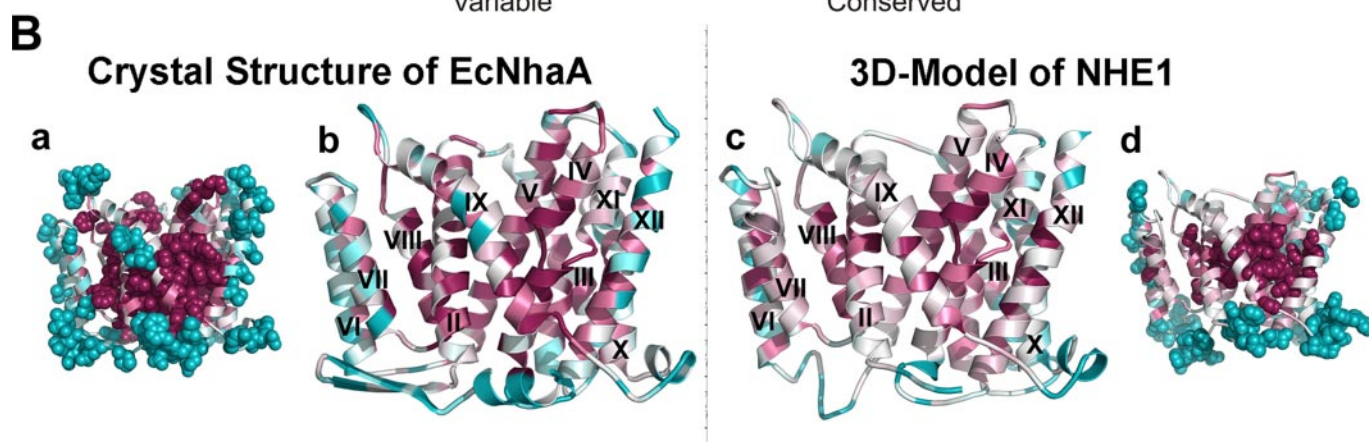
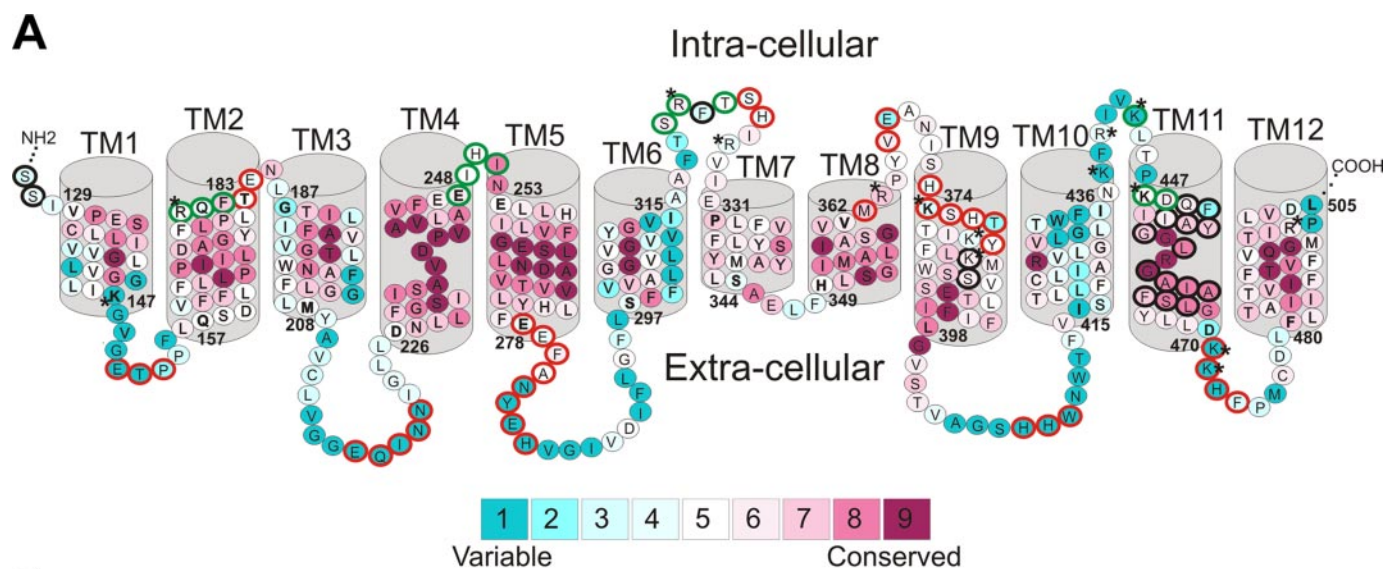


FIGURE 3. Evolutionary conservation profiles of EcNhaA and NHE1. *A*, the novel membrane topology of NHE1 (residues 126–505) that we suggest here. The residues are colored according to their conservation grades using the *color-coding bar*, with *turquoise* through *maroon* indicating *variable* through *conserved*. The start and end residue of each of the TM segments is marked in *bold* and *numbered*. Residues that are located on the same helical face are situated on the same column (every fourth position). It is noteworthy that TM4 and TM11 unwind to form extended peptides within the helices. The results of the substituted cysteine accessibility analysis (9) are projected on the topology as follows: residues that are accessible to the intra- or extracellular medium are marked with *green* and *red* circles, respectively. The *thick black circles* mark residues that are completely inaccessible. *Asterisks* denote positively charged residues that are located exterior to the membrane. *B*, the evolutionary conservation profiles of EcNhaA (*left*) and NHE1 (*right*) are mapped on the crystal structure and three-dimensional model, respectively. The intracellular side is facing upward. The amino acids are colored by their conservation grades using the *color-coding bar* as in *A*. TM1 was omitted from the picture for clarity. *b* and *c*, ribbon models of EcNhaA and NHE1 viewed from the membrane. The TM segments are numbered. *a* and *d*, the most variable (score 1) and conserved (score 9) residues are displayed by space-filled atoms. The compatibility of the NHE1 model structure with the phylogenetic profile is evident: the protein core is conserved, whereas the periphery is variable, as with EcNhaA.

variable amino acids (16–18). Accordingly, analyses of evolutionary conservation have been used to predict the structures of membrane proteins (19–22). They have also been exploited to validate model structures (23), as in the present study.

We mapped the conservation scores calculated on the basis of the alignment of 94 sequences comprising the bacterial NhaA Na^+/H^+ antiporter family on the crystal structure of EcNhaA (6) (Fig. 3*B*, *a* and *b*). As expected, the most highly conserved residues are at the inter-helix interfaces within the TM region, whereas the most variable residues are located in the periphery; where they face the lipid membrane and populate the extra-membranal loops. Reassuringly, a very similar pattern was observed for our model structure of NHE1 (Fig. 3*B*, *c* and *d*). The results, obtained using an alignment of 305 Na^+/H^+ exchangers related to NHE1, strongly support our NHE1 model structure.

Interestingly, a cluster of titratable residues (Fig. 4, *A* and *B*), all evolutionarily conserved (Fig. 4, *C* and *D*), is located within the conserved core in the center of the membrane in each of the structures. Titratable residues are very rare in the membrane, presumably because of the large desolvation free energy associated with their transfer from the aqueous phase into the membrane (24, 25). Their presence in the membrane is often associated with function (26). These titratable residues were indeed shown to be essential for the activity of both transporters (27–29) (supplemental data Tables 1S and 2S) and arguably are involved in conformational changes and cation translocation (please see “Discussion” and Fig. 1 for a detailed description of the role of these residues).

The NHE1 Model Structure Is Consistent with the Positive-Inside Rule—Gunnar von Heijne and his co-workers (25) showed that the topology of the vast majority of TM proteins

Three-dimensional Model of NHE1 and Functional Implications

is such that amino acid positions at the intracellular ends are enriched in the positively charged residues, lysine and arginine, relative to the extracellular side. This observation, termed the positive-inside rule, can be used to predict and evaluate the topology of membrane proteins. Analysis of the NHE1 three-dimensional model (incorporating residues 126–505) revealed 12 lysine/arginine residues on the cytoplasmic side and only 3 lysine residues on the extracellular side (Fig. 3A). For reference, EcNhaA includes 16 lysine/arginine residues on the cytoplasmic side and 5 on the extracellular side (6).

The NHE1 Model Structure Is Consistent with Mutagenesis Studies—Classical genetic and biochemical experiments and site-directed mutagenesis studies of eukaryotic Na^+/H^+ exchangers (supplemental data Tables 1S and 2S) have yielded abundant data. For simplicity, we divided these data into two main groups: residues that are essential for function *versus* those that are unessential. Residues were considered essential if their replacement resulted in loss or change of function (*e.g.* ion-translocation and pH-regulation), or if they were shown to be involved in binding of inhibitors.

When these mutagenesis data are projected on the NHE1 model structure, it can be seen that most of the residues defined as essential for activity are located in the core of the TM domain (Fig. 5), which is consistent with their role in maintaining the architecture and function of the transporter. On the other hand, most of the unessential residues face the membrane or are located in the extra-membranal loops. One essential residue, Ser³⁵¹, unexpectedly faces the membrane lipids, and its functional relevance will be discussed below. Residues that participate in pH regulation, and thus mediate cellular signals, are located both on a cytoplasmic loop and within the protein core.

Mutagenesis studies point to 14 residues whose replacement affects the sensitivity of NHE1 to its inhibitors (Table 1S). Some of these mutations do not affect Na^+ affinity, implying that the inhibitor-binding site is physically distinct and suggesting that the inhibitors induce allosteric regulation (30).

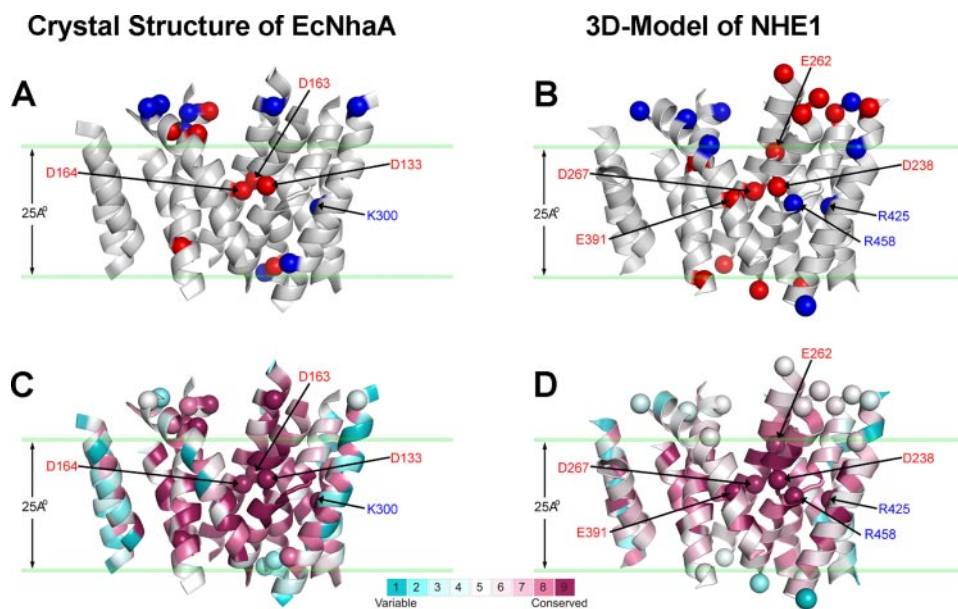


FIGURE 4. Titratable residues in the NHE1 and EcNhaA transporters. A side view of the crystal structure of EcNhaA (6) (A and C) and our model structure of NHE1 (B and D), which are displayed in a ribbon representation with the intracellular region in the upward direction. TM1 and the extra-membranal loops were omitted for clarity. The horizontal green lines mark the approximate boundaries of the hydrocarbon region of the membrane. In panels A and B, the transporters are colored gray, and the locations of the C α atoms of the titratable residues are depicted as spheres. The red spheres correspond to aspartate and glutamate residues, and the blue to arginines and lysines. In panels C and D the amino acids are colored by their conservation grades using the color-coding bar, with turquoise through maroon indicating variable through conserved. Again, the locations of the C α atoms of the titratable residues are depicted by spheres. It is evident that a central cluster of titratable residues is located in the conserved protein core, suggesting that it plays important functional roles in the transporters.

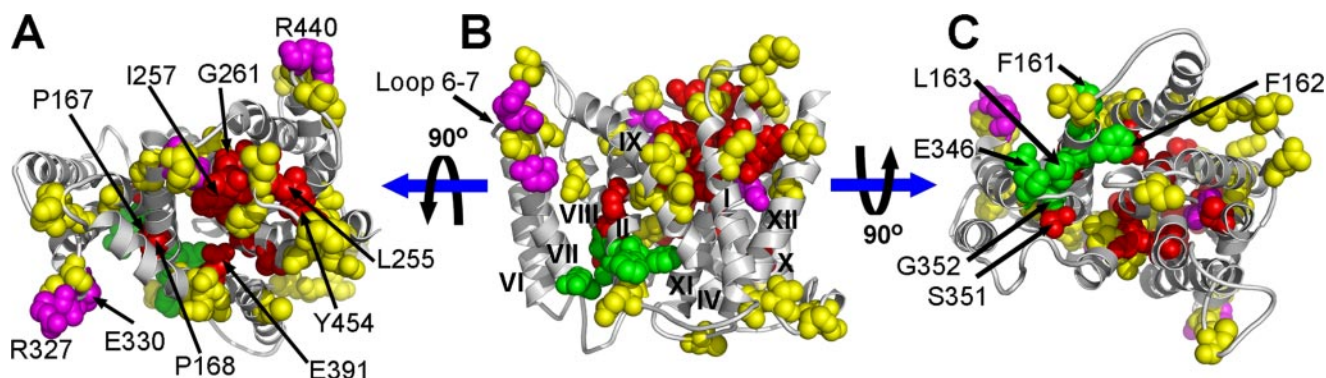


FIGURE 5. Mutagenesis studies in eukaryotic Na^+/H^+ exchangers. The three-dimensional model structure of NHE1 is displayed with gray ribbon and the residues that were mutated are presented using space-filled atoms using colors to represent the experimental outcome. Residues that were implicated in ion translocation (Pro¹⁶⁷, Pro¹⁶⁸, Ser²³⁵, Asp²³⁸, Pro²³⁹, Ala²⁴⁴, Leu²⁵⁵, Ile²⁵⁷, Val²⁵⁹, Phe²⁶⁰, Gly²⁶¹, Glu²⁶², Asn²⁶⁶, Asp²⁶⁷, Thr²⁷⁰, Ser³⁵¹, Glu³⁹¹, Cys⁴²¹, and Tyr⁴⁵⁴) are colored red, residues that are involved in pH regulation (Arg¹⁸⁰, Arg³²⁷, Glu³³⁰, Arg⁴⁴⁰, Gly⁴⁵⁵, and Gly⁴⁵⁶) in magenta, residues comprising the NHE-inhibitors binding site (Phe¹⁶¹, Phe¹⁶², Leu¹⁶³, Glu³⁴⁶, and Gly³⁵²) in green, and unessential residues (Cys¹³³, Gln¹⁵⁷, Pro¹⁷⁸, Glu¹⁸⁴, Cys²¹², Glu²⁴⁸, His²⁵⁰, Leu²⁵⁴, His²⁵⁶, Ser²⁶³, Val²⁶⁹, Val²⁷¹, Phe³²², His³²⁵, Ser³⁵⁹, Asn³⁷⁰, Ser³⁸⁷, Ser³⁸⁸, Ser³⁹⁰, Thr³⁹², Ser⁴⁰¹, Thr⁴⁰², Ser⁴⁰⁶, Asn⁴¹⁰, Lys⁴³⁸, Lys⁴⁴³, Cys⁴⁷⁷, Gln⁴⁹⁵, and Arg⁵⁰⁰) in yellow (for details see Tables 1S and 2S). A, a top view from the cytoplasmic side of the membrane. B, a side view parallel to the membrane with the intracellular side facing upward; the TM segments are numbered. C, a view from the extracellular side.

We focused on residues whose replacement significantly alters sensitivity to NHE inhibitors (*i.e.* by more than 10-fold), and which are likely to be directly involved in the binding. Specifically, mutagenesis implies that the binding site incorporates residues Phe¹⁶¹, Phe¹⁶², and Leu¹⁶³, all located in TM2, and a second region comprising Gly³⁵² of TM8 and Glu³⁴⁶ on its preceding loop (Fig. 5 and Table 1S). These two regions are located close to each other in our model, and Leu¹⁶³ (TM2) is in direct contact with Glu³⁴⁶ and Gly³⁵² (Fig. 5). Moreover, this binding site is situated at the extracellular side of NHE1, in accordance with the location of the inhibitors (31). All in all, our NHE1 model structure is in excellent agreement with the mutagenesis data.

We note that our model was built independently of the mutagenesis data. The final alignment that was used to construct the structural model is very similar to the initial alignments that were obtained using purely computational methods (presented in Fig. 2). Therefore, the projection of the mutagenesis data on models constructed based on these alignments, which are totally independent of prior knowledge regarding the mutations, show similar results (an example is provided in supplemental Fig. 4S).

NHE1 and EcNhaA Share a Similar Inhibitor-binding Site

Mutations that alter the binding affinity of the NHE inhibitors were located in equivalent positions in a few eukaryotic NHE isoforms, implying that these isoforms share a common binding site (Tables 1S and 2S). Thus, we assumed by extrapolation that the AP inhibitor of EcNhaA binds to an equivalent location on EcNhaA. Accordingly, we designed and isolated seven mutations in residues located in TM2 and TM8 of EcNhaA and examined the sensitivity of their Na⁺ or Li⁺/H⁺ activity to AP inhibition (Table 1 and Fig. 6). The Na⁺/H⁺ antiport activity was measured in everted membrane vesicles isolated from EP432 transformed with the plasmids encoding the various mutations. EP432 lacks the chromosome-encoded antiporters (EcNhaA and EcNhaB) and expresses only the EcNhaA variants from a plasmid. Addition of the respiratory substrate, lactate, to these membrane vesicles (*downward-facing arrow* in Fig. 6) resulted in generation of ΔpH, as monitored by quenching of the fluorescence of acridine orange, a fluorescent probe of ΔpH. Addition of either Na⁺ or Li⁺ to the reaction mixture (*upward-facing arrow* in Fig. 6) initiated the Na⁺ or Li⁺/H⁺ antiport activity, as monitored by dequenching of the fluorescence. EP432 transformed with plasmid pAXH (32) or the vector plasmid pBR322 served as positive and negative controls, respectively. To determine the effect of AP on the antiport activity, we added the inhibitor at various concentrations before adding lactate. The half-maximum inhibitory concentration (IC₅₀) of AP was determined as described (5).

Amino acid residues whose mutation changed the sensitivity to AP by at least 3-fold relative to the wild-type were considered to be involved in or affect the AP binding site. Specifically, mutations W62C, F72C, G76C, and H225R exerted no effect on inhibition by AP; the IC₅₀ value was very similar to that of the wild type (1.7 μM). N64C and F71C mutations increased the sensitivity of the Na⁺ but not of the Li⁺ antiport activity to AP inhibition; the IC₅₀ values of AP for these mutants were 0.5 and

TABLE 1
AP sensitivity of EcNhaA mutants

Location of the mutations		IC ₅₀	
		NaCl	LiCl
<i>μM AP</i>			
Wild-type		1.7	2.2
W62C	TM2	1.2	1.5
F71C	TM2	0.3 ^a	0.8 ^b
F72C	TM2	1.8	2.6
G76C	TM2	1.6	1.2
N64C	TM2	0.5	1.7
H225R	TM8	1 ^b	2.3
H225Q	TM8	0.8	7.8

^a IC₅₀ values of AP inhibition in mutants that are different by more than 3-fold than wild-type are bold.

^b For calculation of the IC₅₀ values of AP inhibition, the activity of the antiporter in percent dequenching (100% corresponds to the activity in the absence of AP) was plotted *versus* different AP concentrations as previously described (5). The Na⁺/H⁺ or Li⁺/H⁺ antiporter activity was measured at various ion concentrations around the apparent *K_m* at the pH of maximal activity (pH 8.5 or pH 7.5).

0.3 μM, respectively. In contrast, N64C and H225Q decreased the sensitivity of the Li⁺ but not of the Na⁺ antiport activity to AP inhibition; the IC₅₀ values of AP for these mutants were 17 and 7.8 μM, compared with 2.2 μM for the wild type.

The above results support our conjectured location of binding of the AP inhibitor on EcNhaA. We cannot yet explain why the substitution of Cys for Asn⁶⁴ and Phe⁷¹ increased the sensitivity of the Na⁺ but not of the Li⁺ antiport activity to AP, whereas similar mutations in Asn⁶⁴ and in His²²⁵ decreased the sensitivity of the Li⁺ but not of the Na⁺ antiport activity. We can only speculate that the binding sites of Li⁺ and Na⁺ differ in size, as suggested previously (33) and as predicted from the different sizes of these hydrated cations.

Comparison between Novel and Previously Suggested NHE1 Topologies

Our model, which was derived from sequence alignments with a functional homologue, presents a novel topology. A previously suggested topology, which was based on hydrophobicity scales (9) (Fig. 2), was assessed by substituting cysteines for 83 of the residues of NHE1 and determining the accessibility of these substituted cysteines to cysteine-directed reagents from outside and inside the cell (9). The membrane topology of our model agrees with the experimental findings of Wakabayashi and co-workers (9) (Fig. 3A), mainly in the extracellular loops within TM segments.

The cysteine accessibility analysis (Fig. 3A) yielded conflicting results in two regions, where accessibility to both sides of the membrane was apparent in adjacent residues. The authors suggested that such regions could be inserted into the membrane and might play a role in ion translocation. We believe that this is indeed the case in one of these regions, which in our model is located at the end of TM2 (see "Discussion"). The second region, located in the loop between TM6 and TM7, might play a role in pH regulation (Table 1S and Fig. 5).

Both of the predicted topologies assigned the location of the N and C termini of NHE1 inside the cytoplasm, in accordance with the topology of EcNhaA and experimental evidence (3, 34). However, whereas the first TM segment in our model begins at Val¹²⁹, Wakabayashi and co-workers (9) predicted two additional segments at the preceding N-terminal end (Fig. 2). The

Three-dimensional Model of NHE1 and Functional Implications

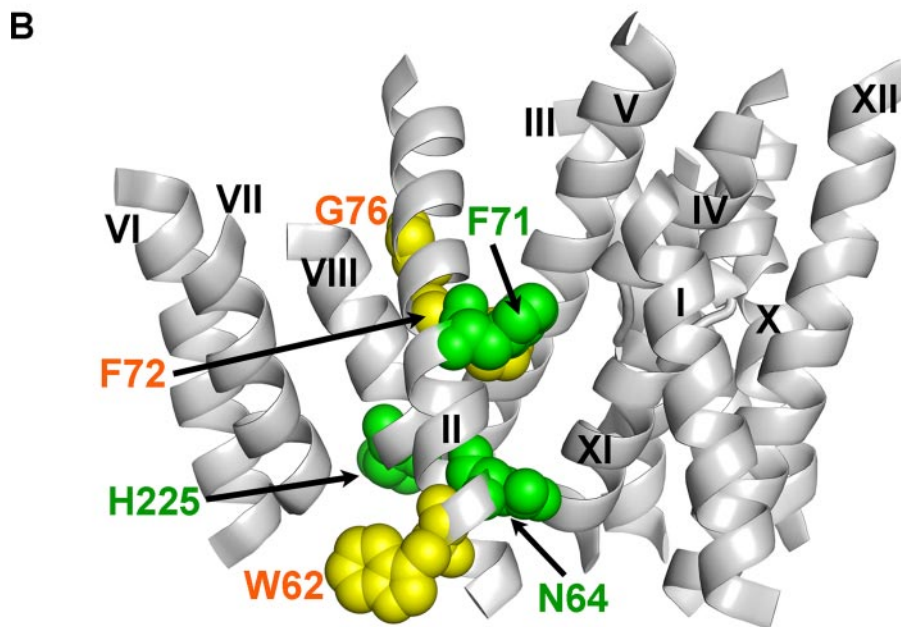
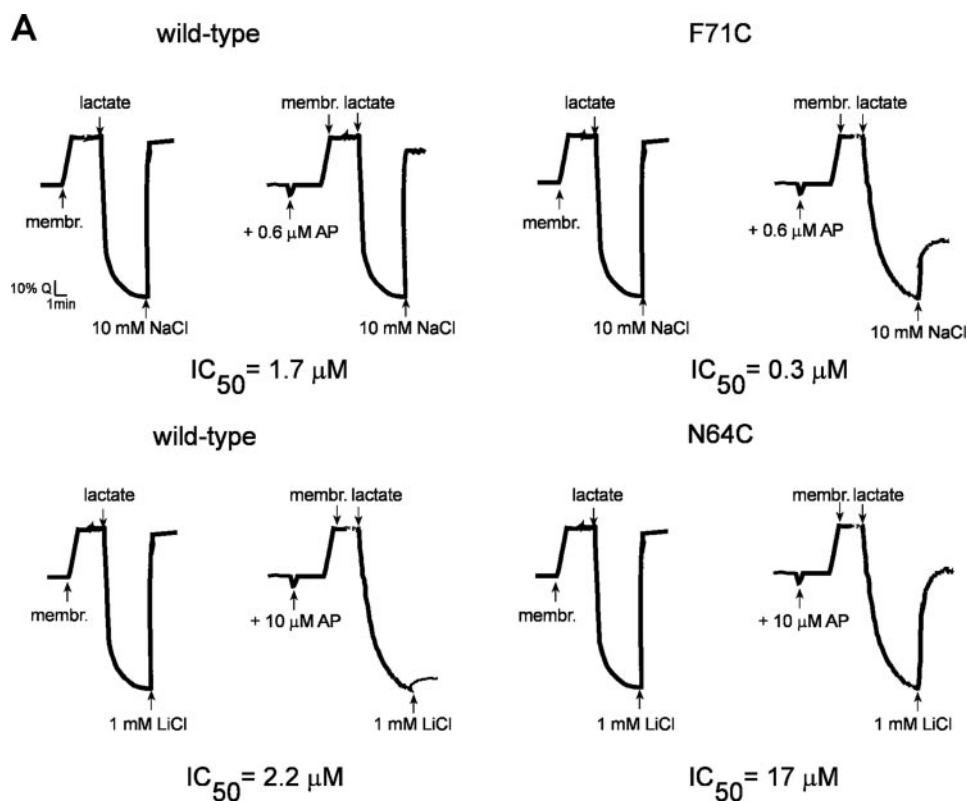


FIGURE 6. The binding site of the AP inhibitor of EcNhaA. *A*, the effect of AP inhibition on the antiporter activity of EcNhaA mutants compared with wild-type. The results obtained for the F71C and N64C mutations showing the most drastic AP effect are displayed. Everted membrane vesicles were isolated from EP432 cells expressing wild-type NhaA or the indicated mutants, and the Na^+/H^+ or Li^+/H^+ antiporter activity was measured at pH 7.5. At the onset of the reaction, membranes were added first and then Tris D-lactate (2 mM) (\downarrow), and the fluorescent quenching (Q) was recorded until a steady state level of ΔpH (100% quenching) was reached. NaCl or LiCl, at the indicated concentrations, was then added (\uparrow), and the new steady state of fluorescence obtained (dequenching) after each addition was monitored. Where indicated, AP, at the indicated concentrations, was added (\uparrow), to the reaction mixture following the addition of the membranes. The experiments were repeated at least three times with practically identical results. Calculated IC_{50} is shown for each experiment. *B*, the crystal structure of EcNhaA (6) is displayed in a gray ribbon representation. Space-filled atoms represent residues that were examined for their involvement in AP binding (Table 1). Residues that play a role in mediating AP inhibition (Asn⁶⁴, Phe⁷¹, and His²²⁵) are colored green, whereas naïve residues (Trp⁶², Phe⁷², and Gly⁷⁶) are colored yellow.

N-terminal segment of NHE1 was suggested to serve as a signal sequence (35), and consistently with that suggestion our evolutionary conservation analysis disclosed that this region (the first ~110 residues) is highly variable among Na^+/H^+ exchangers, and in some of them is even missing. Chymotryptic cleavage of the N-terminal region (residues ~1–150), following expression of NHE1, indeed had little effect on transport activity (34). On the other hand, the first two TM segments in EcNhaA are important and play a role in regulation (6). The second TM is also involved in the formation of the funnels putatively involved in cation-translocation (6). We therefore suggest that, in NHE1, the first two hydrophobic stretches detected by Wakabayashi and co-worker (9), do not correspond to the first two segments in EcNhaA. One possibility is that NHE1 contains two additional TM segments at the N terminus comparing to EcNhaA; these segments might be part of the signal peptide that is truncated in the mature protein.

As shown in Fig. 2, although the previously suggested topology (9) contained two extra TM segments at the N terminus, the next six predicted TM helices overlap with our model. Similarly, within the two topologies the last three helices coincide (Fig. 2). The remaining three segments (TM7–TM9) differ between the topologies. TM7 and TM8 in our model are predicted to be short (14 residues) relative to the other segments (19–27 residues). In contrast, the ninth TM segment predicted by Wakabayashi and co-workers (9) is of normal length, and encompasses roughly these two short TM segments. This assignment is presumably due to the constant size of the window that is used in common hydrophathy plots.

The intracellular region that follows TM8 in our model unexpectedly displays residues that are accessible to external reagents, followed by inaccessible residues (TM9) and then again by residues accessible to external reagents (the extracellular

loop between TM9 and TM10). Wakabayashi and co-workers (9) resolved this inconsistency by assigning an intra-membrane span instead of a transmembranal one (Fig. 2). An intra-membrane span in this region was also suggested for the *Arabidopsis thaliana* Na⁺/H⁺ exchanger isoform 1 (AtNHX1) (35). Alternatively, it is possible that the intracellular loop between TM8 and TM9 participates in ion translocation and is therefore accessible to external reagents. Our model structure is consistent with the latter possibility. A more detailed comparison of the two alternative membrane topologies is provided in supplemental data.

DISCUSSION

Technical difficulties in experimental determination of the membrane topology and three-dimensional structure of NHE1 prompted us to use computational tools to predict its structure based on the crystal structure of the prokaryotic EcNhaA antiporter. This is not a simple undertaking because of the extremely low sequence identity between these two proteins, and necessitated manual integration of the results of various computational tools. The resulting NHE1 model structure is supported by evolutionary conservation analysis and empirical data, as elaborated under "Results," suggesting that it represents a fair approximation of the real structure of this protein. In addition, we located the binding site for inhibitors in both NHE1 and EcNhaA. The finding that the NHE1 and EcNhaA transporters, from human and bacteria, respectively, share a common binding site for inhibitors provides strong support for our contention that the three-dimensional structure of the former can be based on the crystal structure of the latter, despite their low sequence similarity.

Functional Implications of the Model

Similarity to EcNhaA—The most notably conserved helices in both NHE1 and EcNhaA are TM2, TM4, TM5, TM8, and TM11, all located in the protein core (Fig. 3). We suggest below that the similarity in conservation patterns of the two proteins, as well as the equivalent locations of functionally important sites within them (Fig. 4), indicate that they share similar transport mechanisms.

The TM4 and TM11 Assembly Lays the Core of an Alternating-access Mechanism—EcNhaA includes an assembly of the TM4 and TM11 segments, both unwinding to form extended peptides in the center of the helix, which cross each other in the middle of the membrane (6). These irregular structures form dipoles that are stabilized by two titratable residues located on TM4 (Asp¹³³) and TM10 (Lys³⁰⁰) (6) (Fig. 4, A and C). Their positions are conserved in bacterial NhaA Na⁺/H⁺ antiporters as aspartate and lysine residues, respectively, and were shown to be essential for activity (27–29). In the NHE1 model structure the corresponding positions include, respectively, the essential Asp²³⁸ (Table 2S) and Arg⁴²⁵ (Fig. 4B), which are highly conserved among NHE1-related Na⁺/H⁺ exchangers (Fig. 4D) as aspartate and arginine residues, respectively, and can also compensate for the helix dipoles. In addition, the region predicted to unwind within TM11 in NHE1 contains two essential and conserved glycine residues (Table 1S). Glycines are not favored in helical structures, and their presence in

this region of the model structure might facilitate unwinding of the TM11 helix. Another conserved and potentially charged residue, Arg⁴⁵⁸, is located on TM11 of NHE1 (Fig. 4, B and D). Its mutations to cysteine abolishes expression of NHE1 (9), implying that it is structurally important.

EcNhaA displays two funnels that were suggested to lay the ion-transport path (6). One funnel, open to the cytoplasm, is formed by the cytoplasmic parts of TM2, TM4, TM5, and TM9. The other, open to the periplasm, is formed by the periplasmic parts of TM2, TM8, and TM11. Both funnels are blocked in the middle of the membrane near the TM4–TM11 assembly, and do not form a continuous pore (6). Hunte and co-workers (6) suggested that conformational changes following pH activation presumably allow two alternating conformations of the cation-binding site at the bottom of the funnels. They pointed out that the TM4–TM11 assembly might lay the core of the alternating-access mechanism, as the extended peptides in the middle of the membrane and their dipoles are eminently capable of subtle and rapid conformational changes in response to activation (6).

We suggest that the TM4–TM11 assembly plays a similar role in NHE1 because of its high conservation and the clustering of essential residues within these segments, both critical factors in maintaining the structure, ion transport, cation specificity and selectivity, and pH regulation of eukaryotic Na⁺/H⁺ exchangers (Tables 1S and 2S).

TM2 Shapes the Path of Cation Transport—TM2 contributes to the formation of the two funnels that are suggested to lay the path for cation transport (6, 29) (Fig. 1B). The crystal structure of EcNhaA shows a bending of the TM2 helix that is probably important for its structural role. Interestingly, the TM2 segment in our NHE1 model structure contains two proline residues (Pro¹⁶⁷ and Pro¹⁶⁸; Fig. 1B), both of which are essential (Table 1S), and an additional Pro¹⁷⁸ located at the cytoplasmic end. Proline-rich segments correspond to irregular helical structures (24), and the assignment of this helix nicely fits its structural features and supports our model structure. In this respect, it is noteworthy that a peptide that corresponds to TM2 in our model (previously known as TM4), and which was studied using high-resolution NMR spectroscopy, displayed irregular structural properties (36). TM2 of EcNhaA, on the other hand, lacks proline residues, and the kink might be driven by local or long-range tertiary interactions (37). Specifically, Yohannan *et al.* (37) proposed "an evolutionary hypothesis" in which some non-proline kinks in TM proteins were first induced by a proline, and during evolution, substitutions in neighboring residues locked the kink within the structure, even when the proline was mutated (37). Overall, the location of TM2 in our model structure, in combination with the mutagenesis data showing that substitutions of residues located on this segment result in a nearly inactive protein in many cases (Tables 1S and 2S), implying that this segment might lay the cation-transport path, as suggested (36).

Residues in TM5 Serve as the Cation-binding Site—TM5 is located spatially close to TM4 and TM11 and displays exceptionally high evolutionary conservation, mainly in residues facing the TM4–TM11 assembly, both in EcNhaA and NHE1 (Fig. 3). Extensive mutagenesis within TM5 in NHE1 demonstrated its importance for expression and targeting to the membrane

Three-dimensional Model of NHE1 and Functional Implications

(30), in accordance with its strategic location in the protein core in our model.

In EcNhaA, this helix includes two titratable residues, Asp¹⁶³ and Asp¹⁶⁴ (Fig. 4, A and C). These residues, which are located in the middle of the membrane, are evolutionarily conserved in the bacterial NhaA Na⁺/H⁺ antiporters as aspartate residues, are essential, and are considered to be the cation-binding site (6, 28). According to our model structure, the corresponding residues in NHE1 are Asn²⁶⁶ and Asp²⁶⁷, respectively. These residues are highly conserved as asparagine and aspartate residues, respectively, within the family of NHE1-related Na⁺/H⁺ exchangers. Asp²⁶⁷ is located at the bottom of the cytoplasmic funnel (Fig. 1B) and, by conjecture, is involved in cation binding; a negative charge at this position is indeed crucial for function (30), and even a mild substitution abolishes the activities of NHE1 and its yeast homologue sod2 (Tables 1S and 2S).

Is TM5 Responsible for the Different Stoichiometries in EcNhaA and NHE1?—We postulate that replacement of the negatively charged Asp¹⁶³ in EcNhaA by the neutral residue Asn²⁶⁶ from NHE1 is important for the observed difference in Na⁺:H⁺ stoichiometry between these two transporters (1:2 in EcNhaA and 1:1 in NHE1). According to our hypothesis, Asp¹⁶⁴ in EcNhaA or Asp²⁶⁷ in NHE1 serves to alternately bind Na⁺ or H⁺ (Fig. 1). On the other hand, Asp¹⁶³ in EcNhaA binds the second proton, whereas its equivalent in NHE1, Asn²⁶⁶, does not participate in cation binding. Nevertheless, because Asn²⁶⁶ is conserved, essential (Table 1S), and facing adjacent helices, we suggest that it might be of structural importance. Further mutations of these residues in both EcNhaA and NHE1 are likely to shed some light on their role in determining the Na⁺:H⁺ stoichiometry of the transporters. However, it is important to note that both of these residues are facing the neighboring helix, contacting other residues, and that they are essential for function (6, 28) (supplemental Table 1S). Thus, it might not be trivial to convert the stoichiometry by a single mutation. We assume that the long evolutionary time between the two organisms allowed substitutions in residues surrounding Asp¹⁶³/Asn²⁶⁷ that maintained the structural integrity of the transporters while inducing the stoichiometry change. Converting the stoichiometry between the organisms, if possible, might therefore require mutations in the neighboring residues as well.

Titratable Residues, Unique to NHE1, Putatively Involved in Ion Translocation—Besides Asn²⁶⁶ and Asp²⁶⁷ discussed above, another acidic residue in TM5, namely Glu²⁶², was also shown to be crucial for the function of NHE1 and its yeast homologue, sod2 (Tables 1S and 2S). This residue is fully conserved as glutamate in NHE1-related Na⁺/H⁺ exchangers, and its proximity to the cytoplasm (Fig. 4, B and D) suggests that it might attract protons following cellular acidification (Fig. 1A).

Glu³⁹¹ (TM9), which faces the cytoplasmic funnel, spatially close to the TM4–TM11 assembly (Fig. 4, B and D), might play a role in the ion-translocation pathway. This position is conserved in NHE1-related Na⁺/H⁺ exchangers, where it is largely occupied by glutamate but also by either asparagine or glutamine. Substitution of glutamine for Glu³⁹¹ in NHE1 significantly reduced activity but did not abolish it (Table 1S), implying that this residue is important in NHE1 but is not the main

binding site. Overall, a cluster of three conserved acidic residues (Glu²⁶², Asp²⁶⁷, and Glu³⁹¹) is located within the core of NHE1 (Fig. 4, B and D), and we suggest that it facilitates the binding and translocation of the cations in this transporter, whereas Asp²⁶⁷, located at the bottom of the cytoplasmic funnel, serves as the main cation-binding site (Fig. 1).

TM8 Plays a Role in NHE1 Activity—TM8 is highly conserved both among the bacterial NhaA Na⁺/H⁺ antiporters and among NHE1-related Na⁺/H⁺ exchangers (Fig. 3). Within this short helix, it is especially noteworthy that His²²⁵ in EcNhaA and its equivalent Ser³⁵¹ in NHE1 (Fig. 5), despite their conservation and polarity, face the membrane. This observation is especially interesting in view of the demonstration by mutagenesis analyses that different substitutions in His²²⁵ shift activity to more acidic pH (H225R), or to more alkaline pH (H225D), or abolish the activity of EcNhaA completely (H225A) (4, 38). Rotation of TM8 by ~180° would place the side chains of His²²⁵ in EcNhaA, and Ser³⁵¹ in NHE1, in the external funnel. We therefore suggest that activation of these transporters involves rotation of TM8 around its axis, such that these residues can participate in cation transport (Fig. 1).

Ser³⁵¹ in NHE1 and its adjacent neighbor Gly³⁵², which is essential in NHE1 (Table 1S), are both highly conserved in NHE1-related Na⁺/H⁺ exchangers, mostly as serine and glycine residues. Currently, there are no reports on mutations in Ser³⁵¹ in the human NHE1, yet this position was shown to be essential in other eukaryotic Na⁺/H⁺ exchangers (Table 2S). Interestingly, our evolutionary conservation analyses showed substitutions of aspartate residues for both Ser³⁵¹ and Gly³⁵² in a fungi-specific clade of plasma membrane Na⁺/H⁺ exchangers. The aspartate pair was shown to be important for activity in several of these transporters (Table 2S). The unique identity of these residues implies a specific trait that is attributed to fungi exchangers, *e.g.* in mediating cation transport, and supports the importance of TM8 for activity.

Putative Exchange Mechanism in NHE1

The scheme in Fig. 1A summarizes the suggested alternating-access mechanism for Na⁺/H⁺ exchange in NHE, and Fig. 1B highlights the location of the main residues that are implicated in the exchange. Overall, the mechanism, which involves consecutive transformations between pairs of conformations that are at chemical equilibrium, is driven by the concentration gradients of sodium or protons across the membrane. The cation-transport path is formed by two discontinuous funnels comprised of TM2, TM4, TM5, and TM9 at the cytoplasmic side and TM2, TM8, and TM11 at the extracellular side. Upon activation by intracellular acidification, a proton, possibly attracted by Glu²⁶² (TM5), enters the cytoplasmic funnel and binds to Asp²⁶⁷ (TM5) located at the bottom of the funnel (*state 2* in Fig. 1A). Conformational changes, induced by the TM4–TM11 assembly, which might include rotation of TM8 by ~180°, then shield the proton from the cytoplasm. Alternatively, an external path now opens to the extracellular matrix (*state 3* in Fig. 1A), which is enriched with sodium. A sodium ion can now compete with the proton for binding to the extracellular site, possibly mediated by Ser³⁵¹ (TM8) (*state 4* in Fig. 1A). Binding of sodium favors the movement to the alternative

conformation, which shields the sodium cation from the extracellular matrix and opens the path to the cytoplasm (*state 5* in Fig. 1A). The sodium can then be released and replaced by a proton, again in accordance with the chemical gradient of these cations (*state 2* in Fig. 1A), and the cycle continues. We note that in accordance with our hypothesis, cysteine scanning mutagenesis on Ser³⁵¹ showed inhibition by the cysteine-directed reagent MTSET.⁴ Further mutagenesis experiments on Ser³⁵¹ and Gly³⁵² in the human NHE1 could help in understanding the importance of TM8 to the transport activity.

Concluding Remarks

Herein, we offer a structural model for NHE1, and propose an alternating-access mechanism (Fig. 1A). The structural model enables correlation between essential residues in NHE1 and their molecular role in the function of the transporter. The suggested mechanism was mainly derived from information pertaining to the bacterial antiporter (6), and also proposes novel mechanistic details. For example, we suggest a role for TM8 in cation translocation and point to the direct involvement of TM2 in the cation path. Our model structure of NHE1 is supported by phylogenetic and published empirical data available for NHE1 and other eukaryotic Na⁺/H⁺ exchangers, specifically pertaining to the protein core (TM2, TM4, TM5, TM8, and TM11). These central segments are evolutionarily conserved and include essential residues in the NHE1 and EcNhaA transporters. Moreover, both transporters display a cluster of titratable residues in the center of the conserved protein core (Fig. 4) that are essential (Tables 1S and 2S) and are presumably involved in conformational changes and cation translocation. Thus, we are fairly confident of the correctness of our model structure of the core of the NHE1 transporter.

On the other hand, we note that the location of the peripheral TM segments TM1, TM3, TM6, TM7, TM9, TM10, and TM12 in the model structure might be approximate, and that the conformations of the extra-membranal loops are tentative. Additional structural data, *e.g.* from high-resolution cryo-EM and x-ray crystallography, are needed to further our knowledge of these regions. Nevertheless, the results of this study demonstrated that even a model structure, particularly when integrated with experimental data, can be used to propose testable hypotheses that will ultimately shed light on function and regulatory mechanisms. They might also pave the way to structure-based drug design, yielding additional NHE1 inhibitors of clinical benefit.

REFERENCES

- Slepkov, E. R., Rainey, J. K., Sykes, B. D., and Fliegel, L. (2007) *Biochem. J.* **401**, 623–633
- Orlowski, J., and Grinstein, S. (2004) *Pflugers Arch.* **447**, 549–565
- Wakabayashi, S., Fafournoux, P., Sardet, C., and Pouyssegur, J. (1992) *Proc. Natl. Acad. Sci. U. S. A.* **89**, 2424–2428
- Padan, E., Bibi, E., Ito, M., and Krulwich, T. A. (2005) *Biochim. Biophys. Acta* **1717**, 67–88
- Dibrov, P., Rimon, A., Dzioba, J., Winogrodzki, A., Shalitin, Y., and Padan, E. (2005) *FEBS Lett.* **579**, 373–378
- Hunte, C., Screpanti, E., Venturi, M., Rimon, A., Padan, E., and Michel, H. (2005) *Nature* **435**, 1197–1202
- Brett, C. L., Donowitz, M., and Rao, R. (2005) *Am. J. Physiol.* **288**, C223–C239
- Forrest, L. R., Tang, C. L., and Honig, B. (2006) *Biophys. J.* **91**, 508–517
- Wakabayashi, S., Pang, T., Su, X., and Shigekawa, M. (2000) *J. Biol. Chem.* **275**, 7942–7949
- Mayrose, I., Mitchell, A., and Pupko, T. (2005) *J. Mol. Evol.* **60**, 345–353
- Landau, M., Mayrose, I., Rosenberg, Y., Glaser, F., Martz, E., Pupko, T., and Ben-Tal, N. (2005) *Nucleic Acids Res.* **33**, W299–W302
- Petrey, D., Xiang, Z., Tang, C. L., Xie, L., Gimpelev, M., Mitros, T., Soto, C. S., Goldsmith-Fischman, S., Kernysky, A., Schlessinger, A., Koh, I. Y., Alexov, E., and Honig, B. (2003) *Proteins* **53**, 430–435
- Jaroszewski, L., Rychlewski, L., Li, Z., Li, W., and Godzik, A. (2005) *Nucleic Acids Res.* **33**, W284–W288
- Bateman, A., Coin, L., Durbin, R., Finn, R. D., Hollich, V., Griffiths-Jones, S., Khanna, A., Marshall, M., Moxon, S., Sonnhammer, E. L., Studholme, D. J., Yeats, C., and Eddy, S. R. (2004) *Nucleic Acids Res.* **32**, D138–D141
- Tang, C. L., Xie, L., Koh, I. Y., Posy, S., Alexov, E., and Honig, B. (2003) *J. Mol. Biol.* **334**, 1043–1062
- Briggs, J. A., Torres, J., and Arkin, I. (2001) *Proteins* **44**, 370–375
- Hurwitz, N., Pellegrini-Calace, M., and Jones, D. T. (2006) *Philos. Trans. R. Soc. Lond. B Biol. Sci.* **361**, 465–475
- Fleishman, S. J., Unger, V. M., and Ben-Tal, N. (2006) *Trends Biochem. Sci.* **31**, 106–113
- Fleishman, S. J., Unger, V. M., Yeager, M., and Ben-Tal, N. (2004) *Mol. Cell* **15**, 879–888
- Baldwin, J. M., Schertler, G. F., and Unger, V. M. (1997) *J. Mol. Biol.* **272**, 144–164
- Adamian, L., and Liang, J. (2006) *BMC Struct. Biol.* **6**, 13
- Fleishman, S. J., Harrington, S. E., Enosh, A., Halperin, D., Tate, C. G., and Ben-Tal, N. (2006) *J. Mol. Biol.* **364**, 54–67
- Fleishman, S. J., and Ben-Tal, N. (2006) *Curr. Opin. Struct. Biol.* **16**, 496–504
- Bowie, J. U. (2005) *Nature* **438**, 581–589
- von Heijne, G. (2006) *Nat. Rev. Mol. Cell. Biol.* **7**, 909–918
- Murtazina, R., Booth, B. J., Bullis, B. L., Singh, D. N., and Fliegel, L. (2001) *Eur. J. Biochem.* **268**, 4674–4685
- Galili, L., Herz, K., Dym, O., and Padan, E. (2004) *J. Biol. Chem.* **279**, 23104–23113
- Inoue, H., Noumi, T., Tsuchiya, T., and Kanazawa, H. (1995) *FEBS Lett.* **363**, 264–268
- Kozachkov, L., Herz, K., and Padan, E. (2007) *Biochemistry* **46**, 2419–2430
- Ding, J., Rainey, J. K., Xu, C., Sykes, B. D., and Fliegel, L. (2006) *J. Biol. Chem.* **281**, 29817–29829
- Counillon, L., Noel, J., Reithmeier, R. A., and Pouyssegur, J. (1997) *Biochemistry* **36**, 2951–2959
- Olami, Y., Rimon, A., Gerchman, Y., Rothman, A., and Padan, E. (1997) *J. Biol. Chem.* **272**, 1761–1768
- Kaim, G., Wehrle, F., Gerike, U., and Dimroth, P. (1997) *Biochemistry* **36**, 9185–9194
- Shrode, L. D., Gan, B. S., D'Souza, S. J., Orlowski, J., and Grinstein, S. (1998) *Am. J. Physiol.* **275**, C431–C439
- Sato, Y., and Sakaguchi, M. (2005) *J. Biochem. (Tokyo)* **138**, 425–431
- Slepkov, E. R., Rainey, J. K., Li, X., Liu, Y., Cheng, F. J., Lindhout, D. A., Sykes, B. D., and Fliegel, L. (2005) *J. Biol. Chem.* **280**, 17863–17872
- Yohannan, S., Faham, S., Yang, D., Whitelegge, J. P., and Bowie, J. U. (2004) *Proc. Natl. Acad. Sci. U. S. A.* **101**, 959–963
- Rimon, A., Gerchman, Y., Olami, Y., Schuldiner, S., and Padan, E. (1995) *J. Biol. Chem.* **270**, 26813–26817
- DeLano, W. L. (2002) *The PyMOL Molecular Graphics System*, DeLano Scientific, San Carlos, CA

⁴ L. Fliegel, personal communication.